Evidence for Differences in the Temporal Progress of *Plasmopara viticola* Clades *riparia* and *aestivalis* Airborne Inoculum Monitored in Vineyards in Eastern Canada Using a Specific Multiplex Quantitative PCR Assay

O. Carisse,[1,†] H. Van der Heyden,[2] D. M. Tremblay,[1] P. O. Hébert,[1] and F. Delmotte[3]

[1] Saint-Jean-sur-Richelieu Research and Development Centre, Agriculture and Agri-Food Canada, Saint-Jean-sur-Richelieu, Quebec J3B 3E6, Canada
[2] Compagnie de Recherche Phytodata Inc., Sherrington, Quebec J0L 2N0, Canada
[3] Institut national de la recherche agronomique, Unité Mixte de Recherche 1065, Santé et Agroécologie du Vignoble, F-33883 Villenave d'Ornon, France

Abstract

Four clades of *Plasmopara viticola* isolated from wild and cultivated *Vitis* species were described in 2013. Only *P. viticola* clades *riparia* and *aestivalis* have been detected in eastern Canada. To increase our understanding of the epidemiology of these clades of *P. viticola*, airborne sporangia were monitored with spore samplers at two experimental vineyards from 2015 to 2018 and at 11, 14, and 15 commercial vineyards in 2016, 2017, and 2018, respectively. At each vineyard and in each year, airborne sporangia were assessed three times weekly from grapevine budbreak to harvest. To accurately monitor airborne inoculum, a specific and sensitive quantitative PCR assay for simultaneous quantification of *P. viticola* clades *riparia* and *aestivalis* was developed. At the experimental site, in the vineyard planted with the hybrid grape variety Chancellor, mostly *P. viticola* clade *riparia* was detected. In vineyards planted with multiple grape varieties, airborne sporangia of *P. viticola* clade *riparia* were prevalent at the beginning of the season, whereas *P. viticola* clade *aestivalis* was mostly detected from mid-season to harvest. At the commercial sites, airborne sporangia of *P. viticola* clade *riparia* were more prevalent in 2016, whereas *P. viticola* clade *aestivalis* was more prevalent in 2017 and 2018. The only significant difference between the inoculum progress curves was the time at which 50% of the seasonal inoculum was reached, with an average for the 3 years of 100.8 and 117.9 days since 1 May for *P. viticola* clade *riparia* and clade *aestivalis*, respectively. When airborne sporangium concentrations were expressed as the proportion of the two clades, in general, the proportion of clade *aestivalis* to that of clade *riparia* was low at the beginning of the season and increased to reach approximately 0.9 to 1.0 at the end of the season. These results suggest that both clades of *P. viticola* coexist, but that clade *aestivalis* is predominant and that downy mildew epidemics caused by *P. viticola* clade *riparia* occur 2 to 3 weeks before those caused by clade *aestivalis*.

Keywords: epidemiology, fruit, oomycetes, pathogen detection, small fruits

By global standards, the wine industry of eastern Canada, including Quebec, is small. However, it is rapidly expanding, with new growers planting grapevines (*Vitis* spp.) and establishing vineyards in several regions, most of them organized around "wine routes." This expansion is a response to the demand for locally produced, high-quality wine, but with it comes increasing pressure from diseases such as downy mildew caused by the oomycete *Plasmopara viticola* (Berk & Curt.) Berlese & de Toni. When vineyards are established in northern areas, such as eastern Canada, special attention must be paid to the selection of grape varieties, with the most important criteria being the type of wine to be produced and viticultural characteristics, including expected yield, potential for the grapes to reach maturity within the frost-free period (i.e., bud emergence after latest spring frosts to berry ripening prior to the first killing frost in the fall), and the ability to survive winter conditions (Caffi et al. 2009). Winter hardiness is of foremost importance because the vines

[†]Corresponding author: O. Carisse; odile.carisse@canada.ca

must be able to survive winter temperatures as low as −35°C. Vines with low or moderate winter hardiness must be protected during the winter months using geotextiles or soil from within rows, which adds to production costs (Carisse 2016). Consequently, although it is considered an important factor, disease susceptibility is not at the forefront when growers choose grape varieties.

Downy mildew is considered one of the most important diseases of grapevines worldwide (Gessler et al. 2011). The grape downy mildew pathogen is specific to the genus *Vitis* and originates from North America (Gessler et al. 2011). In eastern Canada, because of the often mild springs with abundant rainfall, conditions that are conducive to disease development, downy mildew has the potential to destroy the entire crop (Carisse 2016; Gessler et al. 2011). Direct losses can result from rotting of inflorescences and clusters, and indirect losses can result from leaf, tendril, and shoot infections and ultimately from premature defoliation. In the context of northern viticulture conditions, premature defoliation may be critical, as it predisposes the vine to winter injuries. Additionally, the quality of wine produced from infected grapes is reduced. In eastern Canada, five to seven fungicide treatments are generally applied according to a calendar schedule or grapevine growth stage schedule in order to manage downy mildew. A number of these sprays, however, are also applied to control other diseases and as insurance against the highly erratic appearance of downy mildew.

Grapevine susceptibility to downy mildew varies significantly among varieties. In general, cultivars of the common grapevine, *V. vinifera*, are highly susceptible, and French-American hybrids such as Vidal blanc or Marquette are moderately susceptible (Gessler et al. 2011). In eastern Canada, unlike in other wine production areas, >60 grape varieties are grown, the majority of which are French-American hybrids. The most commonly grown varieties are Frontenac noir, Seyval blanc, Vidal, and Marquette, representing 10.1, 8.8, 8.6, and 6.2%, respectively, of all varieties grown in the province

of Quebec (Vin Québec, https://vinquebec.com). However, as the industry matures and as climate change continues, the popularity of *V. vinifera* cultivars, such as Pinot noir or Chardonnay, is increasing.

Given the importance of grape downy mildew, the genetic diversity of *P. viticola* populations from Europe, South Africa, China, and Australia has been studied (Delmas et al. 2017; Fontaine et al. 2013; Gobbin et al. 2003a, b, 2006; Hug 2005; Koopman et al. 2007; Li et al. 2016; Matasci et al. 2010; Rumbou and Gessler 2004, 2006, 2007; Rouxel et al. 2012; Taylor et al. 2019; Yin et al. 2014). From these studies, it was concluded that all populations from introduced *P. viticola* have low genetic diversity and a weak genetic structure. *P. viticola* populations are sexual, with mating mostly random at the vineyard level, although fingerprints of clonal propagation are also found (Gobbin et al. 2007; Taylor et al. 2019). In its area of origin (i.e., North America), Rouxel et al. (2013, 2014) studied the genetic diversity of *P. viticola* in relation to *Vitis* hosts and reported that grape downy mildew is caused by a complex of five *P. viticola* clades, three of which occur on cultivated grapes. These are clade *riparia*, mostly found on interspecific hybrids; clade *vinifera*, mostly found on *V. vinifera* cultivars and hybrids; and clade *aestivalis*, mostly found on *V. vinifera*, *V. labrusca* (fox grape), and hybrids. The fourth and fifth clades described by Rouxel et al. (2013) are *quinquefolia* and *vulpina*, respectively found on Virginia creeper (*Parthenocissus quinquefolia*) and frost grape (wild *V. vulpina*). Based on cross-inoculations of the four clades of *P. viticola* and different host sources, including *Parthenocissus quinquefolia*, *V. vinifera*, *V. labrusca*, *V. riparia*, *V. aestivalis*, and the hybrid variety Chancellor, Rouxel et al. (2014) reported complete host specialization on *Parthenocissus quinquefolia* and on *V. riparia* and less complete host specificity on *V. aestivalis*, *V. labrusca*, and *V. vinifera*.

Considering that in eastern Canada, specifically in the province of Quebec, only *P. viticola* clade *riparia* and clade *aestivalis* had been reported (Rouxel et al. 2014), a research program aimed at understanding the significance of the presence of these two clades of *P. viticola* was initiated. As a first step, this study set out to determine whether the relative abundances of *P. viticola* clade *riparia* and clade *aestivalis* in vineyards are constant or variable over time. To this end, a specific quantitative PCR (qPCR) assay for simultaneous quantification of airborne sporangia of *P. viticola* clade *riparia* and clade *aestivalis* was developed. This assay was then used to monitor airborne inoculum at two experimental vineyards and at several commercial vineyards and to investigate the temporal dynamics of airborne inoculum and variations in co-occurrence of *P. viticola* clade *riparia* and clade *aestivalis*.

Materials and Methods

Development of the qPCR assay. P. viticola *sample collection.* On several occasions from 2010 to 2014, sporangia of *P. viticola* were harvested from sporulating lesions found on different grape cultivars grown in vineyards in eastern Canada (Quebec) using a sterile BBL culture swab (Thermo Scientific, Toronto, Ontario, Canada). Swabs were brought to the laboratory and agitated in a 1.5-ml microcentrifuge tube containing 500 µl of isopropanol (Sigma-Aldrich Canada Ltd., Oakville, Ontario, Canada) to dislodge the sporangia from the sampling swab. The obtained suspension was stored at −20°C until use.

DNA extraction. DNA was extracted using Chelex-based protocols as described in Carisse et al. (2009) and adapted for oomycetes in Fall et al. (2015). To obtain the DNA required for Sanger sequencing, a 75-µl aliquot of the sporangium suspension was added to a 2-ml screw-cap tube (Sarstedt Corp. Inc., Nümbrecht, Germany) containing 100 mg of 425- to 600-µm glass beads (Sigma-Aldrich Canada Ltd.). Mechanical lysis of sporangia was achieved in a FastPrep FP120A instrument (MP Biomedicals, Santa Ana, CA) at 4.0 m·s^{-1} for 20 s and then centrifuged for 5 s using a benchtop minicentrifuge. Isopropanol was evaporated under vacuum using a Vacufuge (Eppendorf Canada Ltd., Mississauga, Ontario, Canada) at 60°C for 20 min. Dry lysate was then resuspended in 300 µl of DNA extraction solution consisting of nuclease-free water (Integrated DNA Technologies Inc., Coralville, IA) and 5% Chelex 100 molecular-

biology-grade resin (Bio-Rad Laboratories, Hercules, CA). Tubes were placed in a dry bath at 105°C for 20 min, agitated for 5 s using a vortexer, and centrifuged at 15,000 × *g* for 5 min at 4°C. Supernatants were used as the DNA source for further analysis.

qPCR primers and probe design. Amplicons of the internal transcribed spacer 1 (ITS1) to ITS2 of *P. viticola* isolates collected in this study and from DNA of each *P. viticola* clade provided by Dr. Delmotte (Rouxel et al. 2013, 2014) were obtained using a standard PCR protocol with primer pair PvABCF and PvABCR (Table 1) and sent for Sanger sequencing (Génome Québec Innovation Centre, Quebec, Canada). Sequences of *P. viticola* clade *riparia* and clade *aestivalis* were aligned with sequences from the literature for other *P. viticola* sequences, various *Plasmopara* spp., and other oomycetes (Supplementary Tables S1 and S2). The new qPCR oligonucleotides, PvA set (PvA-ITS1F, PvA-ITS1R, and PvA-ITS1P) and PvB set (PvB-ITS2F, PvB-ITS2R, and PvB-ITS2P) listed in Supplementary Tables S1 and S2, respectively, were designed using Beacon Designer 8.13 software (Premier Biosoft, Palo Alto, CA). The specificity of the qPCR assays was tested on several *Plasmopara* spp., *Phytophthora* spp. *Bremia lactucae*, and the grape pathogens *Botrytis cinerea* and *Erysiphe necator*. The PvA qPCR set was specific to *P. viticola* clade *riparia* and generated a 105-bp amplicon, whereas the PvB qPCR primer set was specific to *P. viticola* clade *aestivalis* and generated a 129-bp amplicon.

Exogenous internal positive control. An exogenous internal positive control (EIPC) was developed in order to validate qPCR results, detect false negatives, and identify experimental errors in the preparation of the qPCR reaction. The EIPC was designed to be amplified in a multiplex reaction along with the targeted *P. viticola* ITS region in each sample. The EIPC fragment EIPC1MT consisted of double-stranded DNA genomic blocks (gBlocks; Integrated DNA Technologies Inc.) designed as described by Fall et al. (2015). Primers EIPC99F and EIPC99R and probe EIPC99P (Table 1) were designed from the EIPC sequence using Beacon Designer 8.13 (Premier Biosoft) and generated a 99-bp amplicon. The EIPC1MT gBlock gene fragment was further incorporated during DNA extraction in the DNA extraction solution and in the dilution solution used for the standard curve preparation at a concentration of 2×10^2 copies·µl^{-1}.

Preparation of P. viticola *sporangia and* P. viticola *rDNA copy standard curves.* Given the need to precisely quantify sporangia of *P. viticola*, we generated a standard curve from mature sporangia. Sporangia of *P. viticola* clade *riparia* and clade *aestivalis* were harvested from fresh sporulating lesions on grape leaves using a truncated disposable 10-ml pipette connected to a vacuum pump. Sporangia were collected in 10-ml tubes by pouring approximately 5 ml of isopropanol (100%) into the truncated pipettes. The sporangium suspensions were filtered through one layer of cheesecloth and concentrations were adjusted to 4×10^4 sporangia·ml^{-1} by counting sporangia under the microscope with a hemocytometer. A total of 3,125 sporangia were then transferred into extraction tubes along with a clean silicone-coated spore trap rod in order to reproduce the same DNA extraction conditions as the spore trap samples. DNA was then extracted using the DNA extraction method described previously. The same extraction tube was used throughout the entire procedure in order to avoid variable losses of DNA during tube changes, repetitive pipetting, and filtrations commonly encountered in commercial kits (Voglmayr and Constantinescu 2008). Sporangium standard curves were constructed by fivefold serial dilutions of the sporangium DNA extract in dilution solution consisting of nuclease-free water, UltraPure Salmon Sperm DNA solution (Thermo Fisher Scientific Inc., Waltham, MA) at 10 ng µl^{-1} and EIPC1MT gBlock gene fragment at 2×10^2 copies·µl^{-1} to obtain concentrations equivalent to 3,125, 625, 125, 25, 5, and 1 sporangia per DNA extract. This standard curve was analyzed in the qPCR instrument as explained below and generated quantification cycle (Cq) values used as the first step to transform the ITS copy number into the sporangia number.

Additionally, amplicons within the ITS region were generated from *P. viticola* DNA extracts (as described previously) using standard PCR procedure and primer pair PvABCF and PvABCR.

Fragments of 981 bp for *P. viticola* clade *riparia* and 978 bp for clade *aestivalis* were purified using the NucleoSpin PCR clean-up kit (Macherey-Nagel GmbH & Co., Düren, Germany) according to the manufacturer's recommendations. Purified products were then quantified using a 2100 Bioanalyzer instrument (Agilent Technologies, Santa Clara, CA) and concentrations were converted to copy numbers, calculated using the following formula: Number of copies = (concentration $\times 6.022 \times 10^{23}$)/(amplicon length $\times 1 \times 10^9 \times 650$). Amplicon concentrations were adjusted at 2×10^9 copies·μl^{-1} as stock solution and pooled to obtain an equal ratio of *P. viticola* clade and clade *aestivalis* in dilution solution. The ITS copy standard curve was obtained by 10-fold serial dilutions of the *P. viticola* ITS amplicon mix in dilution solution to obtain a concentration range from 2×10^5 to 2 copies·μl^{-1}. For both standard curves of each clade, the procedure was repeated five times (five independent replicates). The slope and intercept of both standard curves were obtained from linear regression and the qPCR efficiency was equal to $(10^{-1/\text{slope}} - 1) \times 100$ (Bustin et al. 2009).

Construction of standard curves to estimate the number of spores from the number of ITS copies. To determine the number of sporangia of *P. viticola* from ITS copy number, a three-step regression analysis was performed for each clade. First, a linear regression analysis was used to establish the relationship between Cq values and logarithm of the number of sporangia. A second regression analysis was used to establish the relationship between the Cq values and the logarithm of ITS copy numbers. Finally, linear regression analysis of predicted number of sporangia against predicted number of ITS copies for Cq values of 21 to 32 was conducted.

qPCR conditions. The *P. viticola* qPCR assay involved simultaneous quantification of the targeted *P. viticola* clade *riparia* and clade *aestivalis* ITS along with the exogenous internal positive control EIPC1MT. All qPCR reactions were carried out in an AriaMx real-time PCR system (Agilent Technologies Canada Inc., Mississauga, Ontario, Canada) with the following two-step conditions: 95°C for 5 min, followed by 40 cycles at 95°C for 30 s and 60°C for 30 s. Reactions were prepared in a final volume of 25 μl using the QuantiFast Multiplex PCR +R Kit (Qiagen, Mississauga, Ontario, Canada), final concentrations of 1× QuantiFast Multiplex PCR Master Mix, 100 ng μl^{-1} of bovine serum albumin (New England Biolabs, Ipswich, MA), 400 nM of *P. viticola* qPCR primers, 200 nM of *P. viticola* qPCR probes, 300 nM of EIPC qPCR primers, and 200 nM of EIPC probe. Each qPCR run included 3 μl per reaction of the *P. viticola* clade ITS copies standard curve, 3 μl per reaction of an EIPC control consisting of a sporangia-free silicone-greased rod DNA extract, 3 μl per reaction of DNA extract from airborne spore samples, and a no template control. All reactions were performed in duplicate. Sporangium number for each clade and for each sample was obtained from ITS copy number. Furthermore,

Table 1. List of primers and probes used in this study

Sequence name	Sequence (5′ to 3′)	Description[u]	Target[v]
PvA-ITS1F	GGATCATTACCACACCTAAAAC	qPCR forward primer	*Plasmopara viticola* clade *riparia* ITS1
PvA-ITS1P[w]	AGTT<u>A</u>TCGC<u>T</u>GCC<u>T</u>ATT̲TCAT[x]	qPCR dual-labeled hydrolysis probe	*P. viticola* clade *riparia* ITS1
PvA-ITS1R	TAGCTGCAACCACCGA	qPCR reverse primer	*P. viticola* clade *riparia* ITS1
PvB-ITS2F	GGTTGTTAGACTTTGTGATTAGTAA	qPCR forward primer	*P. viticola* clade *aestivalis* ITS2
PvB-ITS2P[y]	CTC<u>G</u>ACAA<u>A</u>CAAA<u>C</u>CGGGA[x]	qPCR dual-labeled hydrolysis probe	*P. viticola* clade *aestivalis* ITS2
PvB-ITS2R	GGC̲AGAAAGCATA<u>C</u>TATATAAGC	qPCR reverse primer	*P. viticola* clade *aestivalis* ITS2
EIPC99F	ACGAGAATTAAGGTCACTTTC	qPCR forward primer	Exogenous internal positive control EIPC1MT
EIPC99P[z]	TTCTTGCCTGTTCGCCGCTG	qPCR dual-labeled hydrolysis probe	Exogenous internal positive control EIPC1MT
EIPC99R	CCCTTCATACCCGATCTG	qPCR reverse primer	Exogenous internal positive control EIPC1MT
PvABCF	TCAGTCTTGAACGAGGAAT	Standard forward PCR primer	*P. viticola* clades *riparia* and *aestivalis* ITS1 to ITS2
PvABCR	CCGATTGGCTACAGATGA	Standard reverse PCR primer	*P. viticola* clades *riparia* and *aestivalis* ITS1 to ITS2

[u] qPCR = quantitative PCR.
[v] ITS = internal transcribed spacer.
[w] Single-quenched PrimeTime qPCR probe 5′6-FAM/3′IABkFQ.
[x] Underlined nucleotides in probes are locked nucleic acid modified bases.
[y] Single-quenched PrimeTime qPCR probe 5′Cy5/3′IAbRQSp.
[z] Double-quenched PrimeTime qPCR probe 5′HEX/ZEN/3′IABkFQ.

Table 2. Description of the vineyards where airborne sporangia of *Plasmopara viticola* clade *riparia* and clade *aestivalis* were monitored in 2016, 2017, and 2018[z]

Year					
2016		**2017**		**2018**	
Site ID	Variety	Site ID	Variety	Site ID	Variety
HE	Seyval blanc	SBL	Chardonnay	SPA	Frontenac blanc
SR	Seyval noir	HE	Seyval blanc	LB	Riesling
SJA	Pinot noir	SR	Seyval noir	BR1	Vidal
SJE	Lucy Kuhlmann/Bacco noir	SI	Frontenac blanc	BR2	Frontenac blanc
LB	Riesling	SJA	Pinot noir	FA	Chardonnay
SUT	Chardonnay	SJE	Lucy Kuhlmann/Bacco noir	DUO	Marechal Foch
DUV	Marechal Foch	SS	Vidal blanc	DUG	Seyval blanc
DUG	Seyval blanc	SA	Marechal Foch	SE	Chancellor
DUO	Seyval blanc	DUT	Seyval blanc	SAO	Seyval blanc
DUT	Seyval blanc	DUO	Seyval blanc	HE	Seyval blanc
SA	Marechal Foch	DUG	Seyval blanc	HA	Vidal
		DUV	Marechal Foch	SUP	Frontenac blanc
		C0	Chardonnay	SR	Seyval noir
		LB	Riesling	SJA	Pinot noir
				SJE	Lucy Kuhlmann/Bacco noir

[z] *Vitis vinifera*: Bacco noir, Chancellor, Chardonnay, Pinot noir, and Riesling; *V. vinifera* hybrid varieties: Frontenac blanc, Lucy Kuhlmann, Marechal Foch, and Vidal blanc; and non-*V. vinifera* hybrids: Seyval blanc and Seyval noir.

the EIPC Cq values of the samples were compared with those of the control within the same qPCR run. A difference of one or more EIPC Cq values was used to identify biases in the amplification reaction and thus was used as a criterion for rejection of the sample result (Carisse et al. 2009).

Laboratory validation of the P. viticola *qPCR assay.* For DNA extraction from airborne sporangia collected on impaction spore samplers, it was important to recover a maximum of DNA from both clades of *P. viticola* and allow for absolute quantification. Thus, the DNA extraction procedure described above was slightly modified. First, the sampling surface of the spore samplers, which consisted of polystyrene rods coated with silicone grease (Dow Corning, Midland, MI), was collected after field sampling and placed directly in 2-ml screw-cap tubes. To dislodge the sporangia from the silicone grease, 75 μl of isopropanol (100%) was added to each tube prior to the mechanical lysis step. Second, the DNA extraction solution consisted of nuclease-free water, 5% Chelex 100 molecular-biology-grade resin, EIPC1MT gBlock gene fragment at 2×10^2 copies·μl^{-1}, and UltraPure Salmon Sperm DNA solution at 10 ng μl^{-1}. Salmon sperm DNA was used as a carrier to increase the assay sensitivity, especially when starting from samples low in pathogen concentration, and to reduce the nonspecificity of the oligos during the qPCR reaction. Supernatants were maintained at 4°C for a maximum of 1 h and used for qPCR sporangium quantification.

Drops (0.1 μl) of each *P. viticola* clade sporangia suspension in isopropanol (100%) prepared as described above were deposited onto plexiglass (825 UV) rods coated with silicone vacuum grease (Carisse et al. 2009) in order to circumscribe sporangia at the center of the rod and thus facilitate accurate microscopic assessment. Rods

were kept at room temperature for approximately 5 min to allow evaporation of isopropanol, after which the number of sporangia per rod was counted under a light microscope at ×250 magnification. The number of sporangia was then assessed with the DNA extraction and qPCR procedures described above. This procedure was repeated 56 times with different ratios of *P. viticola* clade *riparia* and clade *aestivalis* sporangium numbers per rod, ranging from 0 to 260 and from 0 to 175, respectively. Regression analysis was used to establish the relationship between the number of sporangia assessed by the *P. viticola* qPCR assay and the number of sporangia counted under the microscope.

Monitoring airborne sporangium concentrations of *P. viticola* clades *riparia* and *aestivalis*. *Sampling site description.* Airborne sporangium concentrations (ASCs) of *P. viticola* clade *riparia* and clade *aestivalis* were monitored from 2015 to 2018 at two experimental vineyards located at the Agriculture and Agri-Food Canada experimental farm in Frelighsburg, Quebec, Canada. The first vineyard (vineyard 1) planted with the grape variety Chancellor measured 48 × 48 m, with between-row spacing of 3.0 m and within-row spacing of 0.9 m. This vineyard was separated from other vineyards by at least 100 m. The second vineyard (vineyard 2) planted with the grape varieties Vidal, Chancellor, Geisenheim, and Seyval blanc measured 50 × 30 m, with between-row spacing of 3.0 m apart and within-row spacing of 0.9 m. At the experimental farm, weeds, insects, and diseases were managed in accordance with common practices, except for downy mildew, which was managed with a protectant fungicide (Captan 80WDG at 1.5 kg/ha) only when severity of downy mildew reached 30% leaf area diseased, based on observation of eight vines per vineyard. To determine which clade of *P. viticola* induced downy mildew, sporangia were collected from downy mildew lesions by gently pressing greased sampling rods onto sporulating lesions. Each time, a minimum of 25 lesions was assessed. This procedure was repeated at least three times per season, and the clades of *P. viticola* present were determined using the above-described qPCR assay. ASC of *P. viticola* clade *riparia* and clade *aestivalis* was also monitored at 11, 14, and 15 commercial vineyards in 2016, 2017, and 2018, respectively. The commercial vineyards were located in southwestern Quebec and cover four administrative counties (Brome-Missisquoi, Haut-Richelieu, Les Jardins-de-Napierville, and Haut-Saint-Laurent). The commercial vineyards were managed according to grower standard practices. At all sites (experimental and commercial), ASC was monitored three times per week using one rotating-arm impaction spore sampler placed 45 cm above the ground, generally toward the southeast end of each vineyard, in the direction of the prevailing wind. The samplers ran 50% of the time from 08:00 to 14:00 (local time). After exposure, the number of sporangia per rod was counted using the qPCR assay developed in this study and converted to the number of sporangia per cubic meter of air. Information on sampling site and grape varieties is provided in Table 2.

Analysis of airborne P. viticola *clade* riparia *and clade a*estivalis *inoculum progress curves.* The area under the inoculum progress curves (AUIPC) was calculated using equation 1:

$$AUIPC = \sum_{i}^{n-1} \left(\frac{ASC_i + ASC_{i+1}}{2} \right) \times (t_{i+1} - t_i) \qquad (1)$$

where *n* is the sampling time (*t*) and ASC_i is the ASC at time t_i. Because inoculum production and sampling periods varied slightly for the 3 years, the AUIPC was standardized ($AUIPC_{std}$) by dividing AUIPC by the total duration of sampling in days. To further characterize inoculum progress curves (IPCs), separately for each site and each year, ASCs were transformed to cumulative values and then to the proportion of the maximum cumulative amount of airborne sporangia sampled (PASC) so that the data ranged from 0 to 1. An exponential growth model was then fitted to PASC data. Based on the shape of the PASC curves, different forms of the exponential model were tested (single one, two, and three parameters, and modified one and two parameters). The most appropriate exponential model for all 80 IPCs (for each clade, 11, 14, and 15 IPCs in 2016, 2017, and 2018, respectively) was selected based on randomness
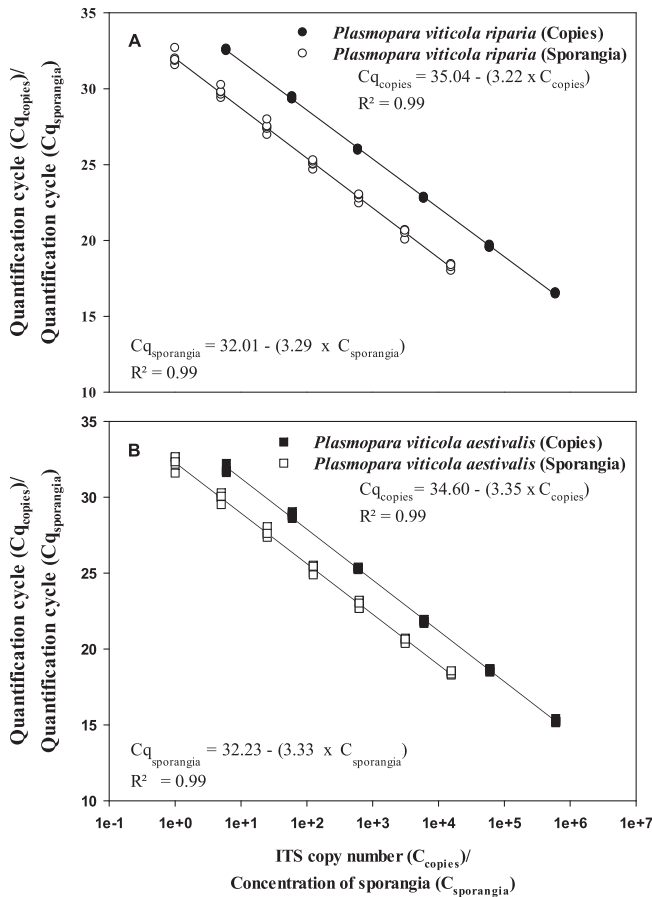

Fig. 1. Relationship between the quantification cycle (Cq) value and the log concentration of **A,** *Plasmopara viticola* clade *riparia* and **B,** *P. viticola* clade *aestivalis* and between the Cq value and the log concentration of internal transcribed spacer 1 (ITS) copies.

and normality of residuals, goodness of fit between predicted and observed values (R^2), and standard deviation around the regression lines. The selected model is shown in equation 2:

$$PASC = Y_0 + a \times e^{b \times t} \qquad (2)$$

where Y_0 is the initial amount of PASC, a is a scaling parameter, b is a shape parameter, and t is the number of days since 1 May. This model was fitted to the data of the 80 IPCs using the SAS statistical analysis program (version 9.4, PROC NLIN, Marquardt method; SAS Institute Inc., Cary, NC). The influence of clade of *P. viticola* on mean ASC, maximum ASC (log ASC + 1), AUIPC$_{std}$, parameters from the exponential model (Y_0, a, and b), and time from 1 May to reach 50% of the seasonal production of airborne sporangia estimated from the exponential models were calculated for each year, and each vineyard was analyzed using a one-way analysis of variance with the clade as the treatment factor.

Seasonal co-occurrence between P. viticola *clade* riparia *and clade* aestivalis. To investigate co-occurrence of *P. viticola* clade *riparia* and clade *aestivalis*, data on ASCs were expressed for each year, each vineyard, and each sampling date as the proportion of the two clades by dividing the total number of sporangia per cubic meter by the number of sporangia per cubic meter for one of the clades. The seasonal nonparametric Mann-Kendall test was used to detect monotonic temporal trends (consistent upward or downward trends) in proportions of *P. viticola* clade *riparia* and clade *aestivalis*. Considering that ASC is a time series expressed as $X = (X_1, X_2, X_3 \dots X_n)$, where X is the proportion of one of the clades and n is the sampling day number, separately for each year and for each clade, the second sampling day data were compared with the first sampling
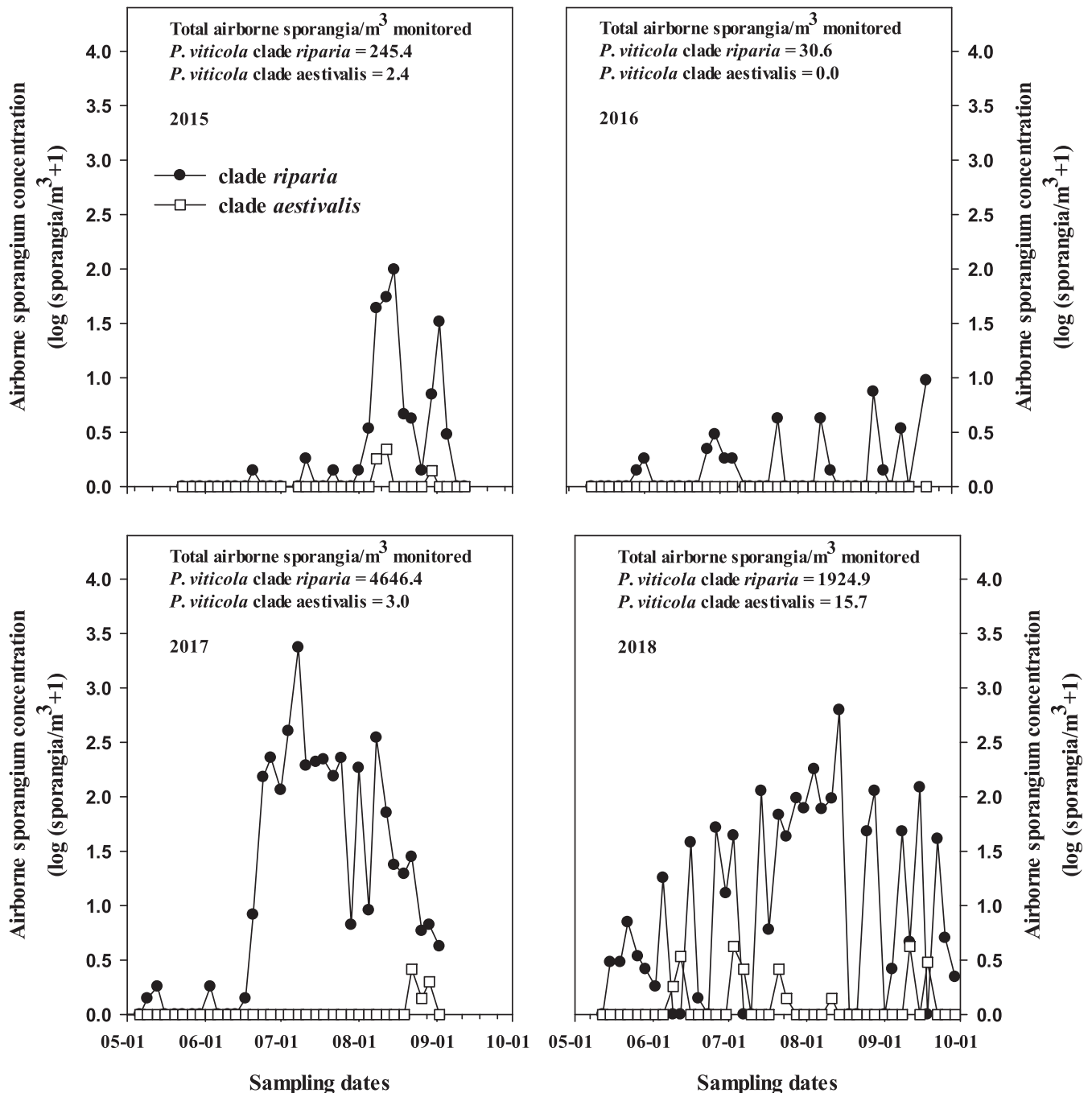

Fig. 2. Temporal progress of airborne sporangia concentrations of *Plasmopara viticola* clade *riparia* (circles) and *P. viticola* clade *aestivalis* (squares) monitored from 2015 to 2018 at experimental vineyard 1 planted with the grape variety Chancellor.

day data, the third sampling day data were compared with the second sampling day data, and so on. The null hypothesis is that there is no temporal trend in the data.

Results

Estimation of the number of sporangia of *P. viticola* clade *riparia* and clade *aestivalis* from ITS copy number. For *P. viticola* clade *riparia*, the amplicon-based standard curve was found to be linear, with efficiency of 104.4%, R^2 of 0.99, a slope of −3.22, and an intercept of 35.04 (Fig. 1A). The sporangia standard curve generated by fivefold serial dilutions of sporangia DNA extractions was also linear, with efficiency of 101.4%, R^2 of 0.99, a slope of −3.29, and an intercept of 32.01 (Fig. 1A). For *P. viticola* clade *aestivalis*, the amplicon-based standard curve was found to be linear, with efficiency of 98.9%, a regression coefficient of 0.99, a slope of −3.35, and an intercept of 34.60 (Fig. 1B). Furthermore, the sporangia sporangium standard curve was also linear, with efficiency of 99.7%, a regression coefficient of 0.99, a slope of −3.33, and an intercept of 32.3 (Fig. 1B). A third linear regression derived from previous standard curve regressions was used to determine the number of ITS copies per sporangium, with an intercept of zero and Cq ranging from 21 to 32. The resulting factors to convert copy number to sporangia were 0.0980 and 0.2137 for *P. viticola* clade *riparia* and clade *aestivalis*, respectively.

The relationship between the number of sporangia deposited onto the rods and counted under a microscope and the number of sporangia estimated with the *P. viticola* qPCR assay was linear, with R^2 values of 0.99 for each clade and intercepts of −1.53 and 0.14 and slopes of 1.15 and 0.99 for *P. viticola* clade *riparia* and clade *aestivalis*, respectively. No signals were detected from rods free of sporangia. The
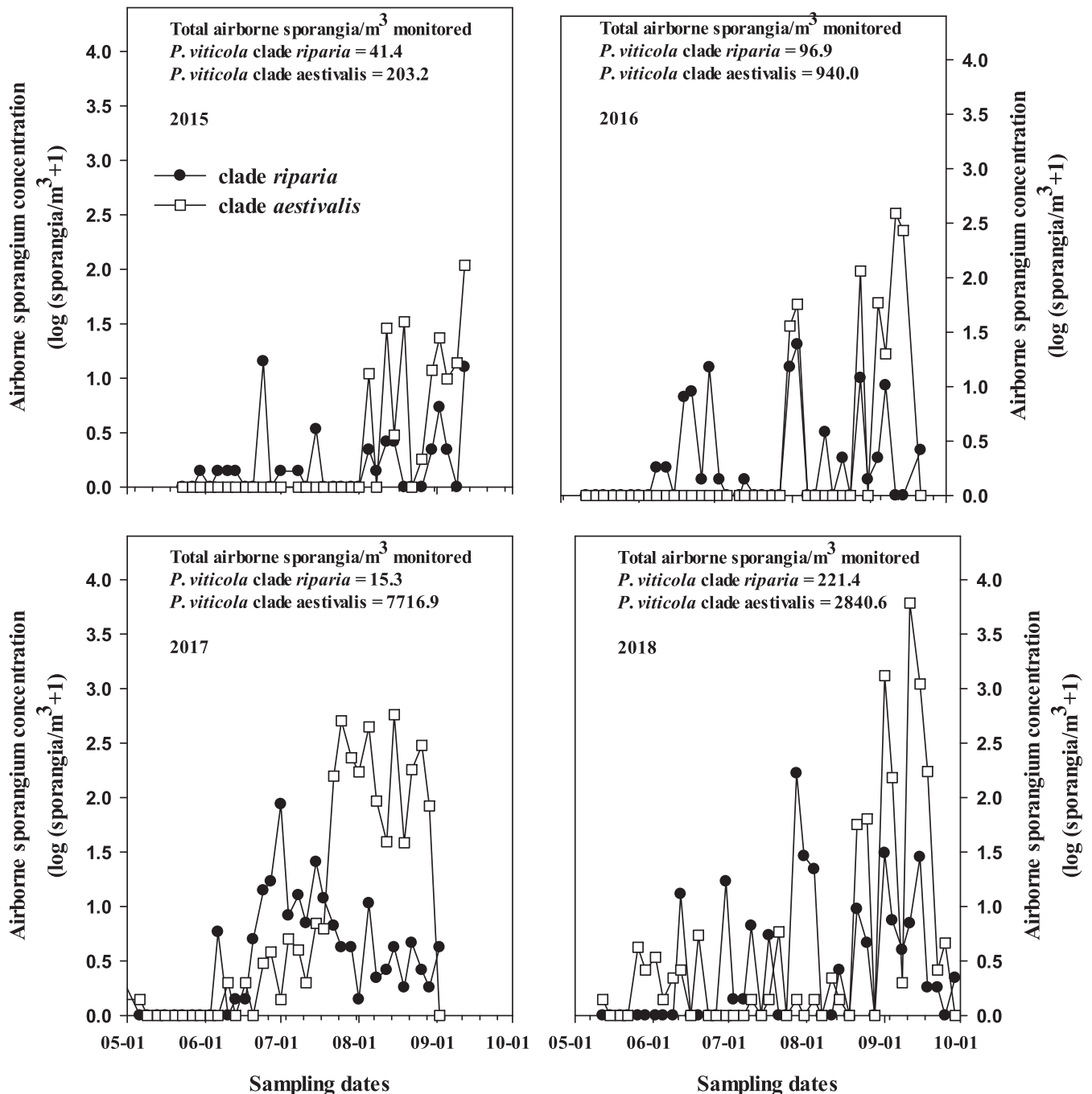

Fig. 3. Temporal progress of airborne sporangia concentrations of *Plasmopara viticola* clade *riparia* (circles) and *P. viticola* clade *aestivalis* (squares) monitored from 2015 to 2018 at experimental vineyard 1 planted with the grape varieties Vidal, Chancellor, Geisenheim, and Seyval blanc.

validation trial confirmed the limit of detection of only one sporangium per reaction for each clade tested. Specificity assays with *Plasmopara* spp., *Phytophthora* spp. *Bremia lactucae*, and the grape pathogens *Botrytis cinerea* and *Erysiphe necator* produced no signal.

Monitoring ASCs of *P. viticola* clade *riparia* and clade *aestivalis*. At the experimental vineyard planted with the grape variety Chancellor (vineyard 1), almost exclusively airborne sporangia of *P. viticola* clade *riparia* were detected during the entire course of the study, with a total of 245.4, 30.6, 4,946.4, and 1,924.9 sporangia m^{-3} during the specific dates in 2015, 2016, 2017, and 2018, respectively (Fig. 2). Only few sporangia of *P. viticola* clade *aestivalis* were collected, with a total of 2.4, 0.0, 3.0, and 15.7 sporangia m^{-3} across the sampling dates in 2015, 2016, 2017, and 2018, respectively (Fig. 2). Indeed, only *P. viticola* clade *riparia* was detected from downy mildew lesions, suggesting that airborne sporangia of clade *aestivalis* collected in air samples originated from nearby vineyard plots. In vineyard 2, planted with the grape varieties Vidal, Chancellor, Geisenheim, and Seyval blanc, both clades were detected from air samples (Fig. 3). In 2015 and 2016, airborne sporangia of *P. viticola* clade *riparia* were more prevalent at the beginning of the season, while clade *aestivalis* airborne sporangia were mostly detected from midseason to harvest (Fig. 3). However, in both 2017 and 2018, airborne sporangia of *P. viticola* clade *aestivalis* were frequently observed throughout the entire growing season (Fig. 3). Regardless of the difference in temporal dynamics of ASCs between the two clades, fewer airborne sporangia of clade *riparia* were collected, with a total of 41.4, 96.9, 15.3, and 221.4 sporangia m^{-3} for sampling dates in 2015, 2016, 2017, and 2018, respectively (Fig. 3). In comparison, 203.2, 940.0, 7,716.9, and 2,840.6 clade *aestivalis* sporangia m^{-3} were collected during sampling in 2015, 2016, 2017, and 2018, respectively (Fig. 3). Indeed, in 2015 and 2016, only clade *riparia* was detected from downy mildew lesions until 1 and 6 August, respectively, after which both clades were detected. In 2017 and 2018, both clades were present on downy mildew lesions at all sampling dates.

At the commercial vineyards, regardless of the clade of *P. viticola*, higher concentrations of airborne sporangia were monitored in 2017 than in both 2016 and 2018, with a total of 106.2, 544.3, and 42.9 sporangia m^{-3} for clade *riparia* and 21.7, 2,473.0, and 924.7 sporangia m^{-3} for clade *aestivalis* on average over sites in 2016, 2017, and 2018, respectively (Table 3). Airborne sporangia of clade *riparia* were detected more frequently in 2016 but less frequently in 2017 and 2018 (Fig. 4). The incidence of commercial vineyards where clade *riparia* and clade *aestivalis* were detected showed that in 2016 and 2017, most vineyards were affected by *P. viticola* clade *riparia* early in the season and that the incidence of vineyards affected by clade *aestivalis* increases progressively toward the end of the season. These observations suggest that there might be some sort of exclusion pattern between the two clades of *P. viticola* and dominance of clade *aestivalis* (Fig. 4).

Analysis of airborne *P. viticola* clade *riparia* and clade *aestivalis* IPCs. Within each year, there were no significant differences in mean airborne sporangia concentration between clade *riparia* and clade *aestivalis*. For the 3 years of the study, there were no significant differences in maximum airborne sporangia concentrations sampled or in AUIPC$_{std}$ between the two clades (Table 3). It was possible to fit the exponential model to the 80 IPCs with R^2 values of >0.85 for 62 IPCs and between 0.71 and 0.84 for the remaining 18 IPCs (Fig. 5). For all three parameters of the exponential model (initial amount of PASC [Y_0], scaling parameter [a], and shape parameter [b]), no significant differences were observed within each year in the values between the two clades, with the exception of parameter b, which was significantly different in 2016 (Table 3). However, the time at which PASC reached 50%, as estimated from the exponential model, differed significantly between the clades for the 3 years of the study (Table 3). The time at which PASC reached 50% was shorter for clade *riparia*, with 105.0, 100.9, and 96.5 days since 1 May in 2016, 2017, and 2018, respectively. For clade *aestivalis*, the time at which PASC reached 50% was 125.6, 117.7, and 110.3 days since 1 May in 2016, 2017, and 2018, respectively. On average for the 3 years, PASC for clade *riparia* reached 50% 17 days earlier than for clade *aestivalis*.

Seasonal co-occurrence between *P. viticola* clade *riparia* and clade *aestivalis*. For each season, based on the Mann-Kendall test, there was a significant temporal trend in the relative proportion of each clade ($P < 0.0001$, 0.0001, and 0.0124 in 2016, 2017, and 2018, respectively). Regardless of the initial proportion of each clade of *P. viticola*, the proportions of *P. viticola* clade *riparia* tended to be high early in the season and decreased toward the end of the season, the populations being replaced by *P. viticola* clade *aestivalis* (Fig. 6).

Discussion

There is no doubt that advances in molecular biology have contributed to modern fungal taxonomy and the discovery of new species, formae speciales, clades, or genotypes of known fungal pathogens. For example, *Botrytis cinerea* was previously believed to be the sole causal agent of gray mold in strawberry and Botrytis bunch rot of grapes. It is now known that these diseases are caused by either one or a complex of *Botrytis* spp. (Plesken et al. 2015; Walker et al. 2011). Similarly, based on genetic and morphological analysis, Rouxel et al. (2013) demonstrated that grape downy mildew is caused by a complex of cryptic genotypes (clades). Proper pathogen identification is the foundation of disease management. However, for the *P. viticola* clades described in 2013, little is known about their interactions with their host or with the environment. It is therefore difficult to know whether management strategies should be adapted to their presence or proportion in the pathogen populations.

This study is one of the first steps toward understanding the epidemiological significance of the *P. viticola* clades described in 2013, specifically those found in eastern Canada. In a previous study,

Table 3. Variables used to compare the temporal dynamics of airborne sporangia concentrations (ASCs) of *Plasmopara viticola* clade *riparia* and clade *aestivalis* in commercial vineyards[y]

Variable[z]	2016		2017		2018	
	Clade *riparia*	Clade *aestivalis*	Clade *riparia*	Clade *aestivalis*	Clade *riparia*	Clade *aestivalis*
Mean ASC	2.14 (3.06) a	0.45 (0.55) a	11.54 (14.89) a	49.42 (73.04) a	1.01 (1.39) a	22.11 (33.65) a
Maximum log(ASC + 1)	0.69 (0.54) a	0.24 (0.82) a	1.77 (0.64) a	1.54 (1.14) a	0.37 (0.67) a	1.29 (0.89) b
AUIPC	4.03 (5.81) a	0.24 (0.31) a	23.14 (29.73) a	136.10 (205.54) a	1.98 (2.81) a	38.88 (59.10) a
Parameter Y_0	−20.22 (32.72) a	−0.06 (0.01) a	−2.91 (4.23) a	−0.12 (0.07) a	−28.88 (46.18) a	−0.02 (0.03) a
Parameter a	20.19 (32.67) a	0.00 (0.00) a	2.74 (4.20) a	0.04 (0.04) a	28.85 (46.14) a	0.00 (0.00) a
Parameter b	0.04 (0.03) a	0.15 (0.04) b	0.02 (0.02) a	0.04 (0.02) a	0.06 (0.04) a	0.07 (0.02) a
Estimated time for 50% ASC	105.00 (14.18) a	125.60 (2.08) b	100.86 (13.00) a	117.71 (9.35) b	96.47 (14.64) a	110.27 (4.11) b

[y] Within each year, for each variable, values for each clade with the same letter are not significantly different according to a one-way analysis of variance ($P \leq 0.05$). Values in parentheses are the standard deviations or standard errors.

[z] Mean ASC is the mean number of per cubic meter over all sites and all sampling dates. Maximum ASC is the maximum log(ASC + 1), over all sites and all sampling dates. AUIPC is the area under the inoculum progress curve. Parameter Y_0 is the initial amount of the proportion of the maximum cumulative amount of airborne sporangia sampled (PASC), a is the a scaling parameter, and b is the shape parameter of the exponential model (equation 2). Estimated time for 50% ASC is the time in days from 1 May to reach 50% of airborne inoculum as estimated with the exponential model (equation 2).

Mouafo-Tchinda et al. (2020) reported that *P. viticola* clade *aestivalis* is more aggressive than clade *riparia* on the grape variety Vidal, even though the temperature response patterns were similar. Under controlled conditions, at the optimal temperature, clade *aestivalis* showed a 14.3% higher disease incidence and 13.3% higher disease severity, produced 2.3 times more sporangia, and had a slightly shorter latency period compared with clade *riparia* (Mouafo-Tchinda et al. 2020). However, our knowledge of the presence,

occurrence, and temporal dynamics of these clades of *P. viticola* under vineyard conditions is limited. Following the description of new clades of *P. viticola*, Rouxel et al. (2014) studied the composition of *P. viticola* populations from eastern North America, the center of origin of *P. viticola*. On cultivated grapevines, three clades were found: clade *riparia* was isolated from interspecific hybrids, such as Chancellor, Marechal Foch, and Vandal-Cliche; clade *vinifera* was isolated from *V. vinifera* varieties and hybrids; and clade *aestivalis*,
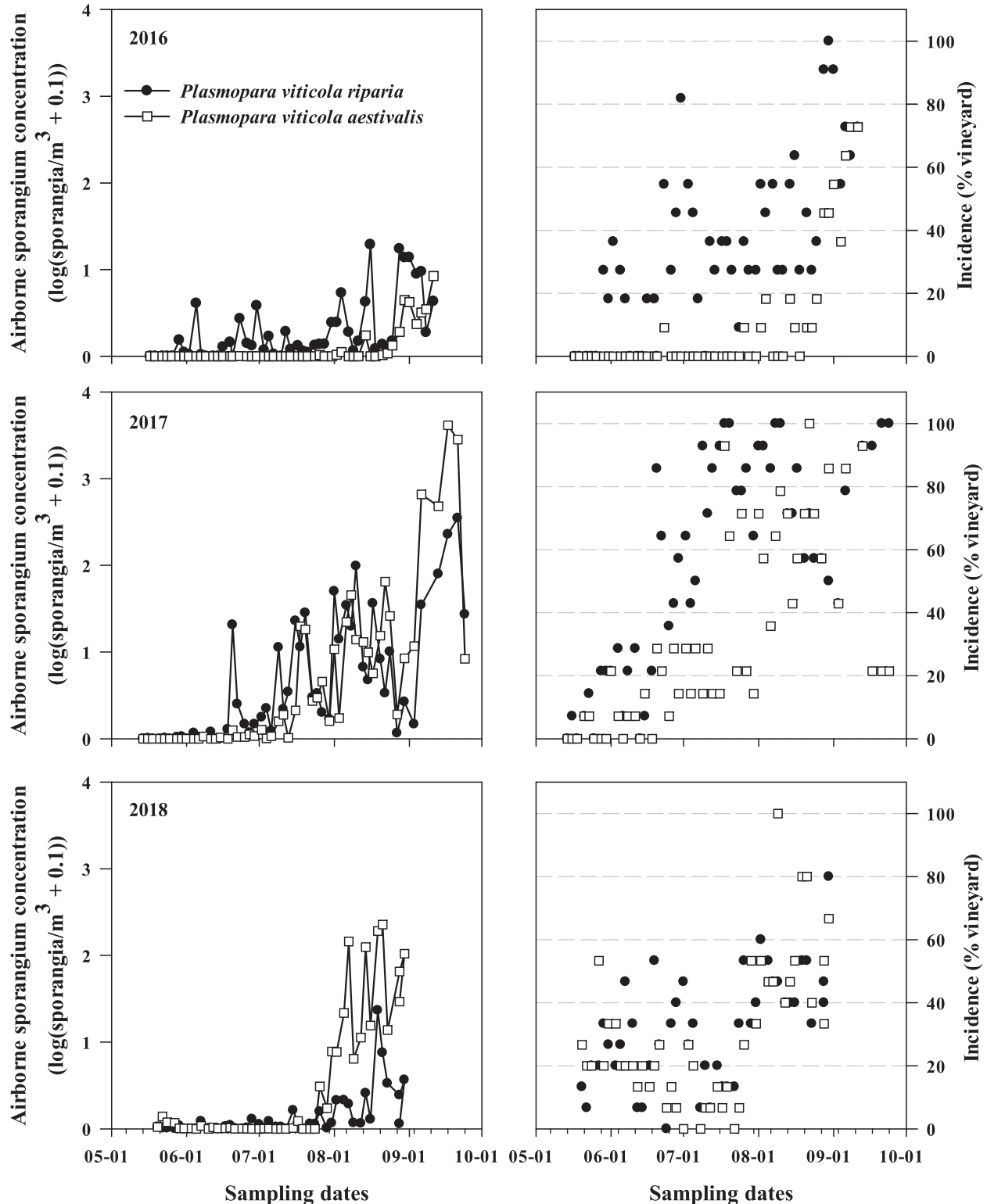

Fig. 4. Temporal progress of airborne sporangia concentrations (left) and incidence (right) of vineyards with detected airborne sporangia of *Plasmopara viticola* clade *riparia* (circles) and *P. viticola* clade *aestivalis* (squares) in 11, 14, and 15 commercial vineyards in 2016, 2017, and 2018, respectively. The list of grape varieties in each vineyard is provided in Table 2.

the most prevalent clade, was found in 83% of the samples collected from infected *V. vinifera*, *V. labrusca*, and hybrids. Hong et al. (2019) reported that *P. viticola* clades *aestivalis*, *vinifera*, and *vulpina* were found in Georgia, whereas clades *aestivalis* and *vinifera* were found in Florida. In both regions, clade *aestivalis* was the most prevalent clade found in 72.1% of the samples, compared with 27.2% for clade *vinifera* and 0.7% for clade *vulpina*. Similarly, studies conducted in Brazil and Western Australia suggested that the population of *P. viticola* in these areas contains only clade *aestivalis* (Camargo et al. 2019; Taylor et al. 2019).

The analysis of the temporal dynamics of airborne sporangia was conducted using the qPCR assay developed in this study, which allowed for reliable quantification of each clade of *P. viticola* from air samples. ASCs are an indirect measure of disease progress and represent populations present in a vineyard even when downy mildew incidence is low (and disease monitoring difficult), thus
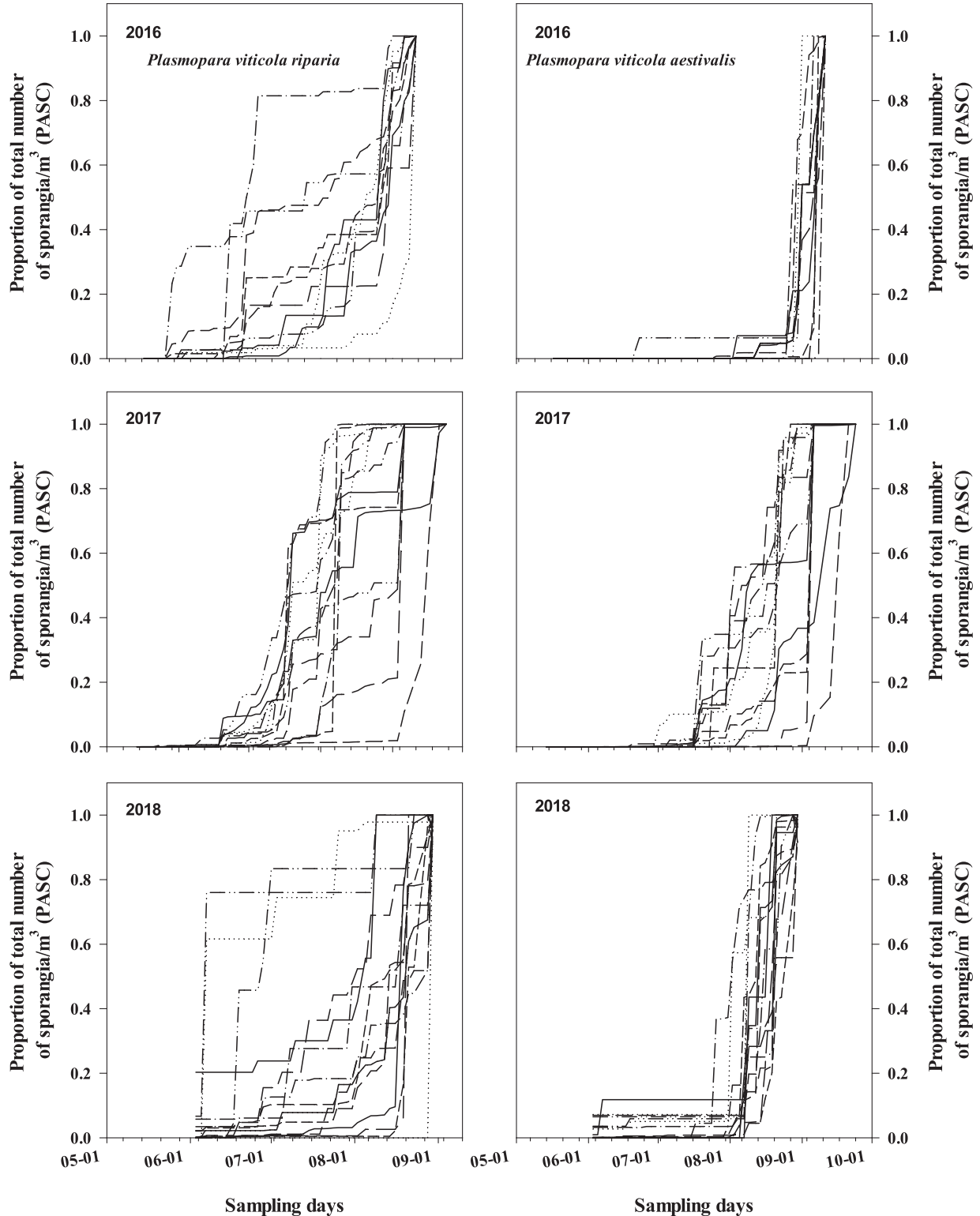

Fig. 5. Inoculum progress curves of *Plasmopara viticola* clade *riparia* (left) and *P. viticola* clade *aestivalis* (right) monitored at 11, 14, 15 commercial vineyards in 2016, 2017, and 2018, respectively. The list of grape varieties in each vineyard is provided in Table 2. PASC = proportion of the maximum cumulative amount of airborne sporangia sampled.

providing appropriate seasonal data. Indeed, at the experimental vineyards, there was good concordance between clades of *P. viticola* identified in the air and from downy mildew lesions. Overall, airborne IPCs for each clade were similar. These observations are in agreement with those reported by Mouafo-Tchinda et al. (2020) whereby the pattern of response of infection and sporulation to temperature is similar for the two clades. However, ASCs were generally higher for clade *aestivalis* than for clade *riparia* (Fig. 4; Table 3). The most important difference between the airborne IPCs was the time to reach 50% of the seasonal inoculum (PASC). On average, it was 100.8 and 117.9 days since 1 May for clade *riparia* and *aestivalis*, respectively, for the 3 years of the study (Table 3). In practice, this means that clade *riparia* epidemics may begin >2 weeks earlier than those caused by clade *aestivalis* and could thus indicate that an adaptation of the management plans may be necessary.

The observations reported in this study on temporal co-occurrence of *P. viticola* clade *riparia* and clade *aestivalis* are in agreement with the findings of Mouafo-Tchinda et al. (2020) that clade *aestivalis* is more aggressive than clade *riparia*. Despite spatial, varietal, environmental, and cultural variations, the temporal pattern of the proportion of each clade of *P. viticola* was similar for the 3 years of the study (Fig. 6). Regardless of the initial proportion of each clade of *P. viticola*, in vineyards where both clades were present, a displacement by clade *aestivalis* was observed during the course of one season, as observed in commercial vineyards. This could be explained by the
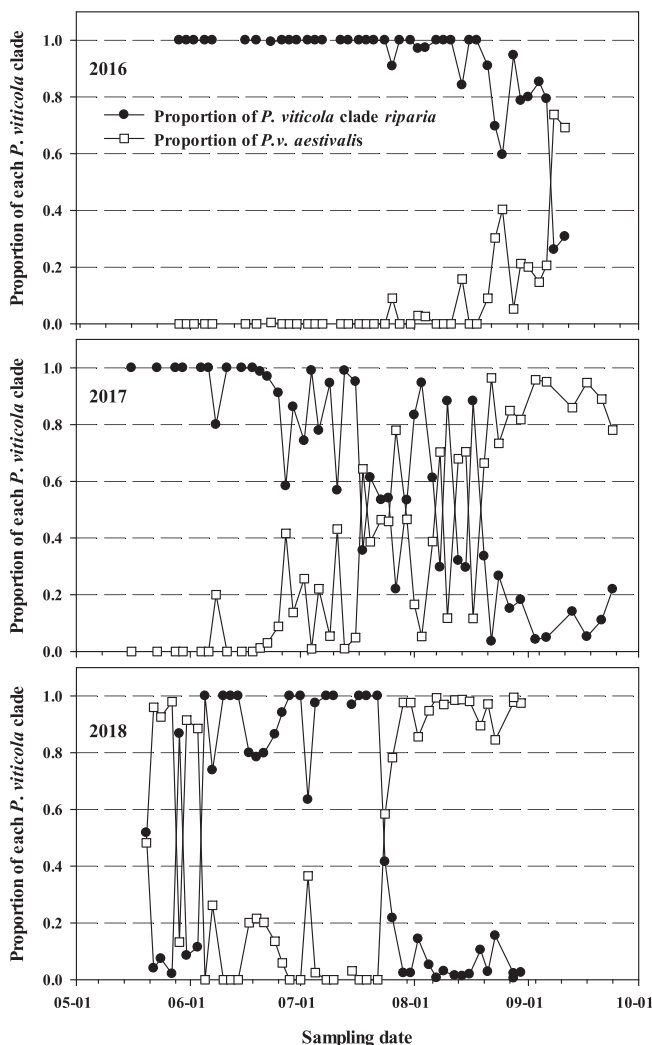
highest production of inoculum and shortest latency period of *P. viticola* clade *eastivalis* (Mouafo-Tchinda et al. 2020). From an ecological perspective, competitive displacement is based on the principle that different species cannot concurrently occupy the same ecological niche, which can be defined in space and time (DeBach 1966). This phenomenon, however, did not completely eliminated clade *riparia*, which was present in most vineyards every year (Fig. 4), suggesting that somehow clade *aestivalis* and clade *riparia* occur in sympatry. Hence, to coexist in the same vineyard, clade *aestivalis* and clade *riparia* must be ecologically distinct in a way that makes intraspecific competition more important for the pathogen population than interspecific competition (Chesson 2000). In other words, clade *riparia* should be able to increase its population even when its proportion in the *P. viticola* population is low (Fig. 6). This phenomenon is known as invasibility and is an essential condition for stable coexistence of species, formae speciales, or clades (Chesson 2000; Siepielski and McPeek 2010).

The observations made in this study clearly showed that *aestivalis* is the predominant *P. viticola* clade present in the province of Quebec, Canada. However, it is expected that the proportion of each clade present in a vineyard or a region varies depending on the grape varieties cultivated. At the experimental site in the vineyard planted with the grape variety Chancellor, only *P. viticola* clade *riparia* was found; at both experimental and commercial sites planted with multiple varieties, both clades were present but airborne inoculum of clade *eastivalis* was highest.

Results also suggest that epidemics caused by *P. viticola* clade *riparia* are occurring earlier than those caused by clade *aestivalis*. Several questions remain. For example, what is the competitive behavior of each clade? Do both clades of *P. viticola* have the same ability to overwinter and the same pattern of oospore maturation (dormancy)? Can both infect grape organs (flowers, berries, leaves, or shoots) in a similar way? Do both clades of *P. viticola* have the same sensitivity to fungicides? Nevertheless, the qPCR assay developed in this study will facilitate research on the ecology of *P. viticola* clade *riparia* and *aestivalis* and monitoring of airborne inoculum, which can be used as a risk indicator for grape downy mildew management.

Fig. 6. Proportion of airborne sporangia of *Plasmopara viticola* clade *riparia* (circles) and *P. viticola* clade *aestivalis* (squares) in 11, 14, and 15 commercial vineyards of the Montérégie region in 2016, 2017, and 2018, respectively. The list of grape varieties in each vineyard is provided in Table 2.

Literature Cited

Bustin, S. A., Benes, V., Garson, J. A., Hellemans, J., Huggett, J., Kubista, M., Mueller, R., Nolan, T., Pfaffl, M. W., Shipley, G. L., Vandesompele, J., and Wittwer, C. T. 2009. The MIQE guidelines: Minimum information for publication of quantitative real-time PCR experiments. Clin. Chem. 55:611-622.

Caffi, T., Rossi, V., Bugiani, R., Spanna, F., Flamini, L., Cossu, A., and Nigro, C. 2009. Evaluation of a model predicting primary infections of *Plasmopara viticola* in different grapevine-growing areas of Italy. J. Plant Pathol. 91: 535-548.

Camargo, M. P., Hong, C. F., Amorim, L., and Scherm, H. 2019. Cryptic species and population genetic structure of *Plasmopara viticola* in São Paulo State, Brazil. Plant Pathol. 68:719-726.

Carisse, O. 2016. Development of grape downy mildew (*Plasmopara viticola*) under northern viticulture conditions: Influence of fall disease incidence. Eur. J. Plant Pathol. 144:773-783.

Carisse, O., Tremblay, D. M., Lévesque, C. A., Gindro, K., Ward, P., and Houde, A. 2009. Development of a TaqMan real-time PCR assay for quantification of airborne conidia of *Botrytis squamosa* and management of Botrytis leaf blight of onion. Phytopathology 99:1273-1280.

Chesson, P. 2000. Mechanisms of maintenance of species diversity. Annu. Rev. Ecol. Syst. 31:343-366.

DeBach, P. 1966. The competitive displacement and coexistence principles. Annu. Rev. Entomol. 11:183-212.

Delmas, C. E., Dussert, Y., Delière, L., Couture, C., Mazet, I. D., Richart Cervera, S., and Delmotte, F. 2017. Soft selective sweeps in fungicide resistance evolution: Recurrent mutations without fitness costs in grapevine downy mildew. Mol. Ecol. 26:1936-1951.

Fall, M. L., Tremblay, D. M., Gobeil-Richard, M., Couillard, J., Rocheleau, H., Van der Heyden, H., Lévesque, C. A., Beaulieu, C., and Carisse, O.

2015. Infection efficiency of four *Phytophthora infestans* clonal lineages and DNA-based quantification of airborne sporangia. PLoS One 10: e0136312.

Fontaine, M., Austerlitz, F. T., Giraud, T., Labbé, F., Papura, D., Richard-Cervera, S., and Delmotte, F. 2013. Genetic signature of a range expansion and leap-frog event after the recent invasion of Europe by the grapevine downy mildew pathogen *Plasmopara viticola*. Mol. Ecol. 22:2771-2786.

Gessler, C., Pertot, I., and Perazzolli, M. 2011. *Plasmopara viticola*: A review of knowledge on downy mildew of grapevine and effective disease management. Phytopathol. Mediterr. 50:3-44.

Gobbin, D., Bleyer, G., Keil, S., Kassemeyer, H. H., and Gessler, C. 2007. Evidence for sporangial dispersal leading to a single infection event and a sudden high incidence of grapevine downy mildew. Plant Pathol. 56:843-847.

Gobbin, D., Pertot, I., and Gessler, C. 2003a. Genetic structure of a *Plasmopara viticola* population in an isolated Italian mountain vineyard. J. Phytopathol. 151:636-646.

Gobbin, D., Pertot, I., and Gessler, C. 2003b. Identification of microsatellite markers for *Plasmopara viticola* and establishment of high throughput method for SSR analysis. Eur. J. Plant Pathol. 109:153-164.

Gobbin, D., Rumbou, A., Linde, C. C., and Gessler, C. 2006. Population genetic structure of *Plasmopara viticola* after 125 years of colonization in European vineyards. Mol. Plant Pathol. 7:519-531.

Hong, C. F., Brewer, M. T., Brannen, P. M., and Scherm, H. 2019. Prevalence, geographic distribution and phylogenetic relationships among cryptic species of *Plasmopara viticola* in grape-producing regions of Georgia and Florida, USA. J. Phytopathol. 167:422-429.

Hug, F. 2005. Genetic structure and epidemiology of *Plasmopara viticola* populations from Australian grape growing regions. Diploma thesis, Eidgenossische Technische Hochschule Zurich, Zurich, Switzerland.

Koopman, T., Linde, C. C., Fourie, P. H., and Mcleod, A. 2007. Population genetic structure of *Plasmopara viticola* in the Western Cape Province of South Africa. Mol. Plant Pathol. 8:723-736.

Li, X., Yin, L., Ma, L., Zhang, Y., An, Y., and Lu, J. 2016. Pathogenicity variation and population genetic structure of *Plasmopara viticola* in China. J. Phytopathol. 164:863-873.

Matasci, C. L., Jermini, M., Gobbin, D., and Gessler, C. 2010. Microsatellite based population structure of *Plasmopara viticola* at single vine scale. Eur. J. Plant Pathol. 127:501-508.

Mouafo-Tchinda, R., Beaulieu, C., Fall, M. L., and Carisse, O. 2020. Effect of temperature on the aggressiveness of *Plasmopara viticola* f. sp. *aestivalis* and *P. viticola* f. sp. *riparia* from Eastern Canada. Online publication. Can. J. Plant Pathol. https://doi.org/10.1080/07060661.2020.1758958

Plesken, C., Weber, R. W. S., Rupp, S., Leroch, M., and Hahn, M. 2015. *Botrytis pseudocinerea* is a significant pathogen of several crop plants but often displaced by fungicide-resistant *B. cinerea* strains. Appl. Environ. Microbiol. 81:7048-7056.

Rouxel, M., Mestre, P., Comont, G., Lehman, B. L., Schilder, A., and Delmotte, F. 2013. Phylogenetic and experimental evidence for host-specialized cryptic species in a biotrophic oomycete. New Phytol. 197:251-263.

Rouxel, M., Mestrem, P., Baudoin, A., Carisse, O., Delière, L., Ellis, M. A., Gadoury, D., Lu, J., Nita, M., Richard-Cervera, S., Schilder, A., Wise, A., and Delmotte, F. 2014. Geographic distribution of cryptic species of *Plasmopara viticola* causing downy mildew on wild and cultivated grape in eastern North America. Phytopathology 104:692-701.

Rouxel, M., Papura, D., Nogueira, M., Dezette, D., and Richard-Cervera, S. 2012. Microsatellite markers for characterization of native and introduced populations of *Plasmopara viticola*, the causal agent of grapevine downy mildew. Appl. Environ. Microbiol. 78:6337-6340.

Rumbou, A., and Gessler, C. 2004. Genetic dissection of *Plasmopara viticola* population from a Greek vineyard in two consecutive years. Eur. J. Plant Pathol. 110:379-392.

Rumbou, A., and Gessler, C. 2006. Particular structure of *Plasmopara viticola* populations evolved under Greek Island conditions. Phytopathology 96: 501-509.

Rumbou, A., and Gessler, C. 2007. Greek epidemics of grapevine downy mildew are driven by local oosporic inoculum: A population biology approach. J. Biol. Res. (Thessalon.) 7:3-18.

Siepielski, A. M., and McPeek, M. A. 2010. On the evidence for species coexistence: A critique of the coexistence program. Ecology 91:3153-3164.

Taylor, A. S., Knaus, B. J., Niklaus, J., Grünwald, N. J., and Burgess, T. 2019. Population genetic structure and cryptic species of *Plasmopara viticola* in Australia. Phytopathology 109:1975-1983.

Voglmayr, H., and Constantinescu, O. 2008. Revision and reclassification of three *Plasmopara* species based on morphological and molecular phylogenetic data. Mycol. Res. 112:487-501.

Walker, A. S., Gautier, A., Confais, J., Martinho, D., Viaud, M., Le Pêcheur, P., Dupont, J., and Fournier, E. 2011. *Botrytis pseudocinerea*, a new cryptic species causing gray mold in French vineyards in sympatry with *Botrytis cinerea*. Phytopathology 101:1433-1445.

Yin, L., Zhang, Y., Hao, Y., and Lu, J. 2014. Genetic diversity and population structure of *Plasmopara viticola* in China. Eur. J. Plant Pathol. 140:365-376.